OPEN BOUNDARY CONDITIONS FOR MULTIDIMENSIONAL ELECTRONIC SCATTERING STATES*

Henry K. Harbury† and Wolfgang Porod
Department of Electrical Engineering
University of Notre Dame
Notre Dame, IN 46556

R. Kent Smith
AT&T Bell Laboratories
Murray Hill, NJ 07974-0636

Abstract

The detailed spatial variation of the electronic scattering states in open and unconfined mesoscopic systems is of interest in both the asymptotic far-field regime and the near-field regime in the vicinity of the scattering potential. We are interested in solving the multidimensional effective mass Schrödinger equation for the scattering states which are compatible with the outward Sommerfeld radiation condition. We present our findings in a comparison of two numerical solution methods which implement non-reflecting boundary conditions on an artificial boundary enclosing the multidimensional problem domain and are compatible with standard finite element techniques.

I. INTRODUCTION

It is of interest to study the near-field scattering states in open-boundary multidimensional ballistic structures. The importance of these scattering states is demonstrated in recent scanning tunneling microscope experiments on metals which support a 2DEG by surface state confinement [1,2]. The interference behavior near point scatterers and step edges is directly related to the two-dimensional local density of states of the electronic scattering system. It has also been pointed out [3] that local field effects in mesoscopic scattering systems are closely related to the electronic scattering states, which have been previously studied for Q1D ballistic structures [4] in the near field regime. To this end, we present a comparison of two numerical methods which implement non-reflecting boundary conditions which are compatible with the outward Sommerfeld radiation condition to solve the single-electron effective-mass Schrödinger equation.

II. SOLUTION METHOD

Two methods for implementing non-reflecting boundary conditions (NRBC) on an artificial boundary are presented. The first is an exact method which uses the known far-field solution for the asymptotic scattering state by matching the known partial-wave expansion to the near-field solution on the artificial domain boundary, and likewise matching the boundary normal derivatives. The Schrödinger equation is integrated by parts with the boundary normal derivatives inserted into the surface term which results in a non-local densely coupled boundary. The second NRBC method is an approximate boundary condition formulated from the application of operators which are, by construction, compatible with the outward Sommerfeld radiation condition in the far-field regime. The boundary condition is again inserted into the surface integral term but results in only a local tridiagonally coupled boundary. The model system is presented followed by a brief synopsis of both the non-local exact NRBC and the local approximate NRBC.

*This work has been supported by the Office of Naval Research and the Air Force Office of Scientific Research.
†H.K.H. is grateful for a fellowship from the Center for Applied Mathematics of the University of Notre Dame.

1. Model System

We seek explicit solutions to the multidimensional single-electron effective-mass Schrödinger equation,

$$-\frac{\hbar^2}{2}\nabla\cdot\left[\frac{1}{m^*}\nabla\psi_E(\mathbf{r})\right]+V(\mathbf{r})\psi_E(\mathbf{r})=E\psi_E(\mathbf{r}). \tag{1}$$

A two dimensional domain will be assumed for simplicity, although the method is easily generalized to three dimensional geometries. As shown schematically in Fig. 1, the scattering domain has an artificial boundary at a radius R_0 from the center of the scattering potential which encloses the solution domain, Ω_0. The potential is assumed constant outside the artificial domain boundary in the region labeled Ω_I, and is taken as the zero reference. As indicated in the figure, an electronic flux, injected by some outside source, is incident upon the mesoscopic scattering region, Ω_0. It will be assumed that the wave-function for the incident flux can be described by a plane wave of the form $\psi_{inc}=a\exp[i\mathbf{k}\cdot\mathbf{r}]$, where $k=|\mathbf{k}|=\sqrt{2m^*E/\hbar^2}$.

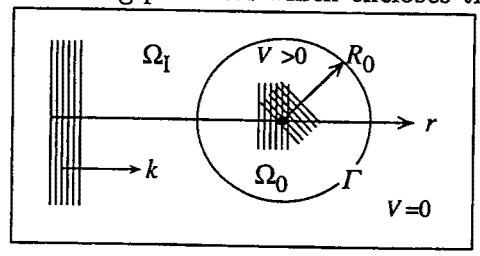

Figure 1. Schematic diagram of the solution domain enclosing the scattering potential.

2. Non-Reflecting Boundary Conditions

In this section a brief synopsis of the exact non-reflecting boundary condition for the solution of Eq. 1 will be presented and the reader is referred to the recent publication [5] by two of the authors for a detailed derivation. The formulation begins with the partial wave expansion of the known far-field solution to Eq. 1,

$$\psi(r\geq R_0,\theta)=\psi_{inc}+\psi_{scatt}=ae^{i\mathbf{k}\cdot\mathbf{r}}+\sum_{m=-\infty}^{\infty}i^m b_m H_m^{(1)}(kr)e^{im\theta}, \tag{2}$$

where a is the amplitude of the incident plane wave, $H_m^{(1)}$ is the Hankel function for the outgoing scattered wave with unknown amplitude b_m. The unknown coefficients, b_m in Eq. 2 may be eliminated through the use of the orthogonality of the angular modes. The known far-field solution is used to obtain the exact normal derivatives of the scattering state on the boundary. The integration by parts of Eq. 1 results in the surface integral term into which this boundary condition is inserted. The resulting formulation using the finite element approximation $\psi\approx\sum_i\psi_i u_i$, where u_i is the i^{th} shape-function, recast into matrix notation has the form of the linear system,

$$[\mathbf{T}+\mathbf{V}+\mathbf{C}]\,\boldsymbol{\psi}=\mathbf{p}, \tag{3}$$

where $\mathbf{T}_{ij}=\frac{\hbar^2}{2}\int_{\Omega_0}\nabla u_i\cdot\frac{1}{m^*}\nabla u_j\,d\Omega$ and $\mathbf{V}_{ij}=\int_{\Omega_0}u_i\,[V-E]\,u_j\,d\Omega$ are the kinetic and potential energy matrix element, respectively, $\mathbf{C}_{ij}=-\frac{\hbar^2}{2}\int_0^{2\pi}u_{i,\Gamma}\frac{1}{m^*}\left[k\sum_{m=-\infty}^{\infty}\frac{H_m^{\prime(1)}(kR_0)}{H_m^{(1)}(kR_0)}\frac{1}{2\pi}\left(\int_0^{2\pi}e^{-im\theta}u_{j,\Gamma}d\theta\right)\times e^{im\theta}\right]R_0d\theta$ is the matrix element which results from the boundary integral, and the right-hand-side vector $\mathbf{p}_i=\frac{\hbar^2}{2}\int_0^{2\pi}u_{i,\Gamma}\frac{1}{m^*}\left[ak\sum_{m=-\infty}^{\infty}i^m\left(J_m'(kR_0)-J_m(kR_0)\frac{H_m^{\prime(1)}(kR_0)}{H_m^{(1)}(kR_0)}\right)e^{im\theta}\right]R_0d\theta$ contains the incident plane wave contribution. The embedded integral around the boundary in $\mathbf{C}$ is inherently non-local and results in a numerical formulation whose discretized boundary is densely coupled.

The approximate non-reflecting boundary condition is based on the method of Bayliss and coworkers [6]. In solving Eq. 1 for the scattering states, a constraint on the artificial boundary is

imposed which restricts the solutions to the class of wave-functions which are compatible with the outward Sommerfeld radiation condition. The boundary constraint is exact in the limit of $R_0 \to \infty$ and has a radially decaying truncation error on the artificial boundary.

In the two-dimensional case, the scattered part of the wave-function may be expanded in the form $\psi_{scatt} \propto e^{ikr} \sum_{j=0}^{\infty} f_j(\theta)/(kr)^{j+\frac{1}{2}}$. A set of linear operators, B_m, compatible with the outgoing Sommerfeld radiation condition are constructed such that on the artificial boundary each m^{th} higher order term is eliminated when B_m operates on the far-field expansion, $B_m \psi_{scatt}|_\Gamma = \mathcal{O}\left(R_0^{-\frac{4m+1}{2}}\right)$. The set of operators are therefore defined as $B_0 = 1$, $B_m = (\partial_r - ik + \alpha_m/r)B_{m-1}$, where α_m is a constant chosen to eliminate the m^{th} term of the expansion. In the two-dimensional case, the first two non-trivial operators are given by:

$$B_1 = (\partial_r - ik + \tfrac{1}{2r}) \quad ; \quad B_1\psi_{scatt}|_\Gamma = \mathcal{O}(R_0^{-5/2}) \tag{4.a}$$

$$B_2 = (\partial_r - ik + \tfrac{5}{2r})B_1 \quad ; \quad B_2\psi_{scatt}|_\Gamma = \mathcal{O}(R_0^{-9/2}). \tag{4.b}$$

Expanding $B_2\psi_{scatt}|_\Gamma$ and implicitly using the original Schrödinger equation, $\frac{\partial^2\psi}{\partial r^2} = -\frac{1}{r}\frac{\partial\psi}{\partial r} - \frac{1}{r^2}\frac{\partial^2\psi}{\partial\theta^2} - k^2\psi$, the result of operating with B_2 on ψ may be rearranged to obtain the boundary normal derivative of the wave-function: $\frac{\partial\psi}{\partial r}\Big|_\Gamma = \left\{\frac{r}{2(1-ikr)}\left[B_2\psi_{inc} + \frac{1}{r^2}\frac{\partial^2\psi}{\partial\theta^2} - \frac{3\psi}{4r^2} + \frac{3ik}{r}\psi + 2k^2\psi\right]\right\}_\Gamma$. Similar to the derivation of the exact non-local NRBC, this boundary normal derivative may be used in the surface term resulting from the integration by parts of Eq. 1. Within the finite element method, the linear system given by Eq. 3 is again obtained, where now the boundary terms are given by $\mathbf{C}_{ij} = \frac{\hbar^2}{2m^*}\frac{4}{3}\eta\int_0^{2\pi}\frac{\partial u_i}{\partial\theta}\Big|_\Gamma\frac{\partial u_j}{\partial\theta}\Big|_\Gamma d\theta + \frac{\hbar^2}{2m^*}(\eta - \xi - 2\gamma)\int_0^{2\pi} u_i\Big|_\Gamma u_j\Big|_\Gamma d\theta$ and $\mathbf{p}_i = \frac{\hbar^2}{2m^*}\left\{-\gamma\int_0^{2\pi} u_i(cos\theta - 1)^2\psi_{inc}d\theta + \xi\int_0^{2\pi} u_i(cos\theta - 1)\psi_{inc}d\theta + \eta\int_0^{2\pi} u_i\psi_{inc}d\theta\right\}$, where ψ_{inc} is the incident wave, $\gamma = \frac{(kR_0)^2}{2(1-ikR_0)}$, $\xi = \frac{3ikR_0}{2(1-ikR_0)}$, and $\eta = \frac{3}{4}\frac{1}{2(1-ikR_0)}$. Unlike the exact NRBC method, this formulation does not contain any embedded integral terms in $\mathbf{C}$ and results in a numerical formulation whose discretized boundary is only tridiagonally coupled. This local NRBC, however, has an approximation error due to the neglected terms of the far-field expansion. This error may be made less than the inherent discretization error in the domain by using a sufficiently large radius.

III. PERFORMANCE

The approximation error of the local NRBC method is expected to improve with increasing radius and approach the exact solution compatible with the outward sommerfeld radiation condition. To compare the two algorithms, it is necessary to fix the discretization error of both the interior domain and the artificial boundary. To this end, a series of regular concentric circular meshes of increasing radius were generated such that the discretization error was held constant by keeping both kh_r and kh_θ equal between grids. The number of nodes was therefore increased with increasing domain radius while keeping the wavevector, k, constant. For the non-local NRBC computations, the infinite sums in the boundary condition were truncated to 40 terms and the linear system, Eq. 3, was solved to obtain the "exact" scattering states. Likewise, the local NRBC was implemented on the same set of problem domains, using the B_2 operator, and the system was solved for the "approximate" solutions. The reflection coefficients, b_m, were obtained from the "exact" solutions and Eq. 2 by integrating around the boundary using the orthogonality of the angular modes. The approximation error of the local NRBC method is determined from $B_m w = B_m(\psi_{scatt} - v)$, where v is the approximate solution computed by enforcing $B_m v = 0$ on the boundary and ψ_{scatt} is the

"exact" formulation of the scattered wave in Eq. 2 using the numerically computed b_m coefficients. Plotted in Fig. 2 is the norm of the computed error of the local NRBC, normalized for the number of nodes on the boundary, for both the B_1 (circles) and B_2 (triangles) operators as a function of increasing domain radius. Each point was obtained from solutions computed using different grids with increasing domain radius. Also shown are the computed fits for the next four higher order terms from Eq. 4.a, $y = c_1(kR_o)^{-5/2} + c_2(kR_o)^{-7/2} + \ldots$, and Eq. 4.b, $y = d_1(kR_o)^{-9/2} + d_2(kR_o)^{-11/2} + \ldots$, which are neglected by the B_1 and B_2 local NRBC approximations, respectively. The local approximation error also improves with increasing wavevector, k, [6] so one may expect better results with higher energy. These results demonstrate that the two NRBC methods approach the same solution at larger radii, neglecting any difference in the discretization error on the boundary. For the non-local method, the accuracy of the embedded boundary integral is sensitive to the number of boundary nodes. For solutions far from the scattering potential, where a large number of nodes must be placed on the boundary, the efficiency of the local NRBC makes it superior to the densely coupled non-local "exact" method. If a given 2-D mesh has N nodes and an effective bandwidth $\beta = \mathcal{O}(\sqrt{N})$, then for the non-local NRBC method the storage requirement is $\mathcal{O}(N\beta)$ non-zero matrix entries as opposed to the tridiagonally coupled local NRBC $\mathcal{O}(N)$ requirement. The difference in storage will also be reflected in the execution time. For the non-local NRBC, the execution time is $\mathcal{O}(N\beta^2)$ for a direct solve and approximately $\mathcal{O}(N\beta)$ for an iterative solution. The local NRBC also has an execution time of $\mathcal{O}(N^2)$ for the direct solve, but the mulplicative constant is much lower. The time for an iterative solve is approximately $\mathcal{O}(N \log N)$, which is feasible for three-dimensional problems.

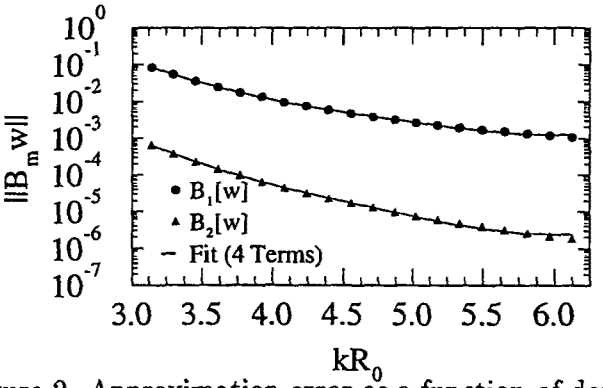

Figure 2. Approximation error as a function of domain radius, R_0, for $B_1 w$ (circles) and $B_2 w$ (triangles). Also shown are the fits for the next few expansion terms.

IV. SUMMARY

Two methods for implementing non-reflecting boundary conditions (NRBC) which are compatible with the outward Sommerfeld radiation conditions were compared for the solution of the single electron effective-mass Schrödinger equation. The exact NRBC results in a non-locally coupled boundary condition whereas the approximate NRBC method is local. The approximation error of the local method, however, requires that the artificial boundary be placed sufficiently far from the scattering center that the neglected higher order terms in the approximation have decayed. The non-local NRBC method has greater accuracy for an artificial boundary placed closer to the scattering potential. The efficiency in both storage and execution time of the local NRBC over the non-local NRBC suggests that, for realistic 3-D problems, only the local NRBC method is feasible.

[1] M. F. Crommie, C. P. Lutz, and D. M. Eigler, *Nature* **363**, 524 (1993).
[2] Y. Hasegawa and Ph. Avouris, *Phys. Rev. Lett.* **71**, 1071 (1993).
[3] R. Landauer, *Z. Phys. B - Condensed Matter* **68**, 217 (1987).
[4] H. K. Harbury, W. Porod, and C. S. Lent, *Superlat. Microstruc.* **11**, 189 (1992).
[5] H. K. Harbury and W. Porod, to appear in *J. Appl. Phys.*, May 15 (1994).
[6] A. Bayliss, M. Gunzburger, and E. Turkel, *SIAM J. Appl. Math.* **42**, 430 (1982).